



Conversion of anilines into azobenzenes in acetic acid with perborate and Mo(VI): correlation of reactivities

C. Karunakaran¹ · R. Venkataraman¹

Received: 27 March 2018 / Accepted: 15 September 2018
© Institute of Chemistry, Slovak Academy of Sciences 2018

Abstract

Azobenzenes are extensively used to dye textiles and leather and by tuning the substituent in the ring, vivid colours are obtained. Here, we report preparation of a large number of azobenzenes in good yield from commercially available anilines using sodium perborate (SPB) and catalytic amount of Na₂MoO₄ under mild conditions. Glacial acetic acid is the solvent of choice and the aniline to azobenzene conversion is zero, first and first orders with respect to SPB, Na₂MoO₄ and aniline, respectively. Based on the kinetic orders, UV–visible spectra and cyclic voltammograms, the conversion mechanism has been suggested. The reaction rates of about 50 anilines at 20–50 °C and their energy and entropy of activation conform to the isokinetic or Exner relationship and compensation effect, respectively. However, the reaction rates, deduced by the so far adopted method, fail to comply with the Hammett correlation. The specific reaction rates of molecular anilines, obtained through a modified calculation, conform to the Hammett relationship. Thus, this work presents a convenient inexpensive non-hazardous method of preparation of a larger number of azobenzenes, and shows the requirement of modification in obtaining the true reaction rates of anilines in acetic acid and the validity of Hammett relationship in the conversion process, indicating operation of a common mechanism.

Keywords Homogeneous catalysis · Kinetics · Oxidations · Structure–reactivity relationships · Azo dyes

Introduction

Azo dyes, a commercially important family of azobenzenes, are pervasively used to dye textiles and leather articles. As a consequence of π -delocalization, the azobenzenes display vivid colors and the color is tuned by the substituent present at the benzene ring (Yamada et al. 2018); the absorption wavelength (λ_{max}) is governed by the Hammett relationship. Merino (2011) has listed various methods of synthesis of azo compounds in her review. Preparation of azobenzenes through aerobic oxidative dehydrogenative coupling of anilines using Au nanoparticles supported on TiO₂ (Grirrane et al. 2008) or Cu–Ag nanoclusters, generated in situ using

Cu(OAc)₂ and Ag₂CO₃ (Seth et al. 2016), or Ag nanoparticles impregnated on carbon (Cai et al. 2013) or Au–Ag alloy nanoparticles on P-, N-, F- and S-doped carbon (Gao et al. 2018) as catalyst have been reported recently. Mesoporous MnO₂ (Dutta et al. 2016) and CuBr₂ or CuBr in pyridine (Zhang and Jiao 2010) also catalyze oxidation of anilines to azobenzenes by air. (Diacetoxyiodo)benzene (Ma et al. 2012) as well as *tert*-butyl hypoiodite (Takada et al. 2012) effectively oxidizes anilines to azobenzenes. The oxidation of anilines to azobenzenes by di-*tert*-butyldiaziridinone requires CuBr as catalyst (Zhu and Shi 2013). Aqueous H₂O₂ oxidizes anilines to azobenzenes but demands perfluorosulfonic acid as catalyst (Paris et al. 2018). The requirement of nanoparticulate precious metals as catalyst (the recovery of which for reuse is a challenge) or uneconomical oxygen source hampers commercialization of the reported research findings. Sodium perborate (SPB, NaBO₃·4H₂O) of anionic formula B₂(O₂)₂(OH)₄²⁻ is a cheap, innocuous, easily handled large scale industrial chemical used as a source of H₂O₂, mainly in detergents (Indi et al. 2017) and mouthwash (Almohareb 2017; Tran et al. 2017). Azobenzenes are prepared in good yield by SPB-oxidation of anilines in glacial

Electronic supplementary material The online version of this article (<https://doi.org/10.1007/s11696-018-0599-z>) contains supplementary material, which is available to authorized users.

✉ C. Karunakaran
karunakaranc@rediffmail.com

¹ Department of Chemistry, Annamalai University, Annamalainagar 608002, India

acetic acid (Karunakaran and Kamalam 2002a). Search of inexpensive, non-toxic, readily available and easily handled catalyst for the said conversion is of interest and Na_2MoO_4 is found to catalyze SPB oxidation of organic sulfides and sulfoxides (Karunakaran and Venkataramanan 2006a, b). The present study shows effective catalysis of SPB oxidation of anilines to azobenzenes by Na_2MoO_4 in acetic acid; molybdenum is an essential trace element for animals and plants. Quantification of the substituent effect on the reaction rate by the Hammett relationship is well established. As the *para*- or *meta*-substituent influences the reaction center and, thus, the reaction rate electronically, Cvijetic et al. (2013) observed parallel correlation of reaction rate with LUMO (lowest unoccupied molecular orbital) energy as well as Mulliken atomic charge. The rate of [4 + 2] cycloaddition of cyclopentadiene with (*E*)-2-aryl-1-cyano-1-nitroethenes, determined by Jasinski et al. (2012), correlates with Hammett constant, σ_p as well as electrophilicity index, ω and the reaction constants are similar. These results confirm that the Hammett substituent constant reflects the electrical characteristics of the substituent. Salter-Blanc et al. (2016) correlation analysis on aniline oxidation by MnO_2 substantiates the same; the oxidation conforms to the Hammett relationship and is governed by the (1) pKa (2) E_{HOMO} (energy of highest occupied molecular orbital) and (3) E_{OX} (oxidation potential). Sun et al. (2018) show operation of linear free energy relationships (LFERs) in the degradation of anilines by K_2FeO_4 in the pH range 6–10. Because of the importance of manufacture of azobenzenes from anilines employing SPB in glacial acetic acid, here we report molybdenum(VI) catalysis of the conversion and correlate the observed reaction rates in terms of Hammett relationship. The results show the routine methodology of obtaining the reaction rates as incorrect and the logically deduced reaction rates conform to the LFER. Further, this study gains interest because amino group on a biomolecule like amino acid, DNA, RNA and protein is responsible for the reactivity and solubility which are determined by acidity or basicity of the medium.

Experimental

$\text{NaBO}_3 \cdot 4\text{H}_2\text{O}$, $\text{Na}_2\text{MoO}_4 \cdot 4\text{H}_2\text{O}$, $\text{Mn}(\text{OCOCH}_3)_2 \cdot 4\text{H}_2\text{O}$, $\text{Fe}(\text{COOH})_2 \cdot 2\text{H}_2\text{O}$, $\text{NiCl}_2 \cdot 6\text{H}_2\text{O}$, $\text{Cu}(\text{OCOCH}_3)_2 \cdot \text{H}_2\text{O}$, $\text{ZrOCl}_2 \cdot 8\text{H}_2\text{O}$, $\text{Cd}(\text{OCOCH}_3)_2 \cdot 2\text{H}_2\text{O}$, $\text{SnCl}_2 \cdot 2\text{H}_2\text{O}$, $\text{Hg}(\text{OCOCH}_3)_2$, $\text{Pb}(\text{OCOCH}_3)_2 \cdot 3\text{H}_2\text{O}$, SbCl_3 , $\text{Bi}(\text{NO}_3)_3 \cdot 5\text{H}_2\text{O}$, $\text{K}_2\text{Cr}_2\text{O}_7$, $\text{Co}(\text{NO}_3)_2 \cdot 6\text{H}_2\text{O}$, $\text{Pd}(\text{OCOCH}_3)_2 \cdot 3\text{H}_2\text{O}$, $\text{K}_2\text{TiO}(\text{C}_2\text{O}_4)_2 \cdot 2\text{H}_2\text{O}$, NH_4VO_3 , $(\text{NH}_4)_6\text{Mo}_7\text{O}_{24} \cdot 4\text{H}_2\text{O}$, Li_2MoO_4 , $\text{Na}_2\text{WO}_4 \cdot 2\text{H}_2\text{O}$, $\text{FeSO}_4 \cdot 7\text{H}_2\text{O}$, $\text{Fe}(\text{NH}_4)_2(\text{SO}_4)_2 \cdot 6\text{H}_2\text{O}$, $\text{Fe}(\text{NH}_4)(\text{SO}_4)_2 \cdot 12\text{H}_2\text{O}$, $\text{Ce}(\text{SO}_4)_2 \cdot 4\text{H}_2\text{O}$, $\text{Ce}(\text{NH}_4)_4(\text{SO}_4)_4 \cdot 2\text{H}_2\text{O}$, $\text{Ce}_2(\text{C}_2\text{O}_4)_3 \cdot 9\text{H}_2\text{O}$, H_3VO_4 , H_2MoO_4 , H_2WO_4 , $\text{H}_3\text{PMo}_{12}\text{O}_{40}$, $\text{H}_3\text{PW}_{12}\text{O}_{40}$, NaOH and trichloroacetic acid, all reagent grade, were used as received. All the anilines used were

of reagent grade. *p*-Iodoaniline and 2,4,6-tribromoaniline were prepared following standard procedures. The anilines purified by distillation, listed with the experimental and literature [given in parenthesis (Buckingham 1995)] boiling points ($^\circ\text{C}$), were: aniline 182 (184), *m*-toluidine 200 (203), *m*-anisidine 249 (251), *m*-chloroaniline 227 (230.5), *m*-bromoaniline 248 (251), *p*-phenetidine 252 (253), *p*-fluoroaniline 180 (184–186), *o,m*-dimethylaniline (2, 3) 220 (221–222), *o,m*-dimethylaniline (2, 5) 212 (213–215), *o,m*-dichloroaniline (2, 3) 250 (252), *o*-toluidine 197 (201), *o*-anisidine 222 (225), *o*-phenetidine 227 (228), *o*-chloroaniline 207 (208.8), *o*-bromoaniline 226 (229), methyl *o*-aminobenzoate 259 (258–261), *o*-aminothiophenol 232 (234), *N*-methylaniline 194 (196) and *N,N*-dimethylaniline 191 (193). The following anilines were purified through recrystallization; the solvent- employed and literature melting points ($^\circ\text{C}$) (Buckingham 1995) are given in parenthesis along with the experimental melting points: *m*-aminophenol 125 (water, 124–126), *m*-nitroaniline 114 (water, 114), *m*-aminobenzoic acid 177 (water, 178), *m*-aminoacetophenone 98 (ethanol, 97–99), *m,p*-dimethylaniline (3, 4) 49 (petroleum ether 40–60, 51), *m,p*-dichloroaniline (3, 4) 71 (ligroin, 72), *p*-toluidine 42 (water, 42–44), *p*-anisidine 56 (petroleum ether 40–60, 57), *p*-aminophenol 184 (water, 186), *p*-chloroaniline 70 (petroleum ether 40–60, 70–71), *p*-bromoaniline 64 (aqueous ethanol, 66), *p*-iodoaniline 67 (petroleum ether 60–80, 67–68), *p*-nitroaniline 147 (water, 148), *p*-aminobenzoic acid 188 (water, 188–188.5), ethyl *p*-aminobenzoate 90 (ethanol, 92), *p*-aminoacetophenone 105 (water, 106), *p*-aminoacetanilide 166 (water, 165–167), sulfanilic acid (water, 25), sulfanilamide 165 (aqueous ethanol, 165–166), *p*-phenylenediamine 145 (ether, 147), *o,m*-dimethoxyaniline (2, 5) 80 (petroleum ether 40–60, 81), *o,m*-dichloroaniline (2, 5) 50 (ligroin, 50), *o,p*-dichloroaniline (2, 4) 63 (ethanol, 63), *o,o,p*-trichloroaniline 78 (ligroin, 78.5), *o,o,p*-tribromoaniline 121 (benzene/ethanol, 122), *o*-phenoxyaniline 45 (ligroin, 45–46), *o*-aminophenol 173 (water, 174), *o*-nitroaniline 71 (water, 72), *o*-aminobenzoic acid 145 (water, 144–148), *o*-phenylenediamine 102 (water, 104), *o,o*-dinitroaniline 141 (ethanol, 141–142) and diphenylamine 53 (ligroin, 52–54). Acetic acid, methanol (analar) and ethanol were purified following standard procedures and distilled for use.

SPB (0.011 mol) and Na_2MoO_4 (0.001 mol) were dissolved in glacial acetic acid (5–7 mL) and aniline (0.015 mol) was added drop-wise or in portions at 50 $^\circ\text{C}$. The temperature was maintained at 50 $^\circ\text{C}$ for an hour. The resultant was poured into water (500 mL) and stirred. The solid was filtered, dried and recrystallized from petroleum ether (40–60 $^\circ\text{C}$).

SPB in glacial acetic acid, with catalytic amount of Na_2MoO_4 , effectively converts many anilines into azobenzenes, identified by their IR (Fig. S1–39 in Supplementary

material) and UV–visible (not presented) spectra and melting points with literature values in parenthesis (Buckingham 1995); the yields are between 70 and 85%. *o*-Aminothiophenol is oxidized, by SPB in acetic acid with Na₂MoO₄, to the corresponding disulfide, identified by its IR spectrum (Fig. S40 in Supplementary material) and melting point. The products of *N*-methylaniline and diphenylamine are likely to be the respective hydroxylamines; the products dissolve in aqueous NaOH and regenerate on acidification. Further, the IR spectra (Fig. S41 and 42 in Supplementary material) show strong broad absorbance around 3425 and 3443 cm⁻¹, respectively, indicating the presence of hydroxyl function. *N,N*-Dimethylaniline oxide is the likely product of *N,N*-dimethylaniline, as seen from its IR spectrum (1650 cm⁻¹; Fig. S43 in Supplementary material). Use of aniline in excess over SPB ensures the absence of overoxidation. The absence of >N→O frequency (ca. 1335 cm⁻¹) in the recorded IR spectra supports the absence of overoxidation and the agreement of the determined melting points with those of the literature values shows the purity of the products.

Substituent, $\bar{\nu}$ (IR), λ_{\max} (UV–vis), mp, yield: H: 1477, 1435 (1480, 1450) cm⁻¹, 439 (443) nm, 68 (71) °C, 80%; *m*-CH₃: 1600, 1485 (1606, 1483) cm⁻¹, 412, 323 nm, 54 (54) °C, 81%; *m*-OCH₃: 1600, 1491 (1594, 1489) cm⁻¹, 312 nm, 80 (74) °C, 83%; *m*-OH: 1515 (1474) cm⁻¹, 323 nm, 71%; *m*-Cl: 1481 cm⁻¹, 417, 321 nm, 103 (103) °C, 82%; *m*-Br: 1458 cm⁻¹, 427, 325 nm, 125 (126) °C, 83%; *m*-NO₂: 1525, 1480 cm⁻¹, 321 nm, 138 (144) °C, 93%; *m*-COOH: 1523, 1459 cm⁻¹, 322 nm, > 280 (340) °C, 84%; *m,p*-Cl₂: 1463 cm⁻¹, 441, 332 nm, 156 (158) °C, 89%; *p*-CH₃: 1598, 1498 (1580, 1483) cm⁻¹, 437, 335 nm, 144 (144) °C, 69%; *p*-OCH₃: 1599, 1506 (1594) cm⁻¹, 421, 313 nm, 87%; *p*-OC₂H₅: 1505, 1469 (1505, 1476) cm⁻¹, 426 nm, 85%; *p*-F: 1497 cm⁻¹, 422, 321 nm, 103 (103) °C, 83%; *p*-Cl: 1477 cm⁻¹, 438, 332 nm, 187 (188) °C, 84%; *p*-Br: 1471 cm⁻¹, 442, 333 nm, 204 (205) °C, 88%; *p*-I: 1467 cm⁻¹, 340 nm, 240 (242) °C, 89%; *p*-NO₂: 1474, 1445 cm⁻¹, 373 nm, 134 (128) °C, 90%; *p*-COOH: 1422 cm⁻¹, 328 nm, > 280 (330) °C, 89%; *p*-COCH₃: 1457 cm⁻¹, 462 nm, 206 °C, 70%; *p*-SO₂NH₂: 1458 cm⁻¹, 450, 328 nm, 25 (25) °C, 80%; *p*-NH₂: 92%; *o,m*-(CH₃)₂ (2, 3), 1472 cm⁻¹, 402, 320 nm, 91%; *o,m*-(CH₃)₂ (2, 5): 313 nm,

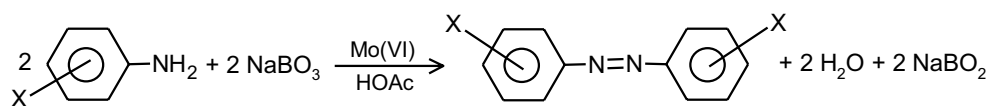
128 (119) °C; *o,m*-(OCH₃)₂ (2, 5): 1508, 1465 cm⁻¹, 436, 312 nm, 75 °C, 83%; *o,m*-Cl₂ (2, 3): 1451 cm⁻¹, 328 nm, 89%; *o,m*-Cl₂ (2, 5): 1459 cm⁻¹, 312 nm, 90%; *o,p*-Cl₂: 1460 cm⁻¹, 323 nm, 90%; *o,o,p*-Cl₃: 1473 cm⁻¹, 344 nm, 95 °C, 90%; *o,o,p*-Br₃: 1454 cm⁻¹, 323 nm, 81%; *o*-CH₃: 1583, 1502 (1580, 1483) cm⁻¹, 390, 314 nm, 54 (54) °C, 87%; *o*-OCH₃: 1459 (1489, 1460) cm⁻¹, 315 nm, 90%; *o*-OC₂H₅: 1585, 1470 (1583, 1476) cm⁻¹, 426 nm; *o*-OC₆H₅: 1478 cm⁻¹, 327 nm, 215 °C, 83%; *o*-OH: 1463 cm⁻¹, 421, 316 nm, 93%; *o*-Cl: 1464 cm⁻¹, 419, 330 nm, 138 (138) °C, 76%; *o*-NO₂: 1428 cm⁻¹, 406, 301 nm, 82%; *o*-COOH: 1443 cm⁻¹, 342, 321 nm, 76%; *o*-COOCH₃: 1487, 1434 (1495, 1440) cm⁻¹, 322 nm, 151 (150) °C, 46%; *o*-NH₂: 1529, 1487 cm⁻¹, 455, 304 nm, 83%; *o*-SH: 1472 (1474) cm⁻¹ (-S-S-), 334 nm, 91 (93) °C, 76%; *o,o*-(NO₂)₂: 1435 cm⁻¹, 422, 318 nm, 138 °C, 92%; -NHCH₃: 3425 cm⁻¹ (>NOH), 333 nm, 135 °C, 71%; -N(CH₃)₂: 1650 (1635) cm⁻¹ (N→O), 306, 256 nm, > 230 °C, 40%; -NHC₆H₅: 3443 cm⁻¹ (>NOH), 80%.

The kinetic runs were made under pseudo-first-order conditions with [aniline] ≫ [SPB] at 20–50 °C. SPB was dissolved in glacial acetic acid, standardized and used immediately. Required weight of Na₂MoO₄ was dissolved in glacial acetic acid in a SMF, diluted stepwise and used without allowing it to stand. Desired concentration of aniline in acetic acid was prepared. Required volumes of the solutions were mixed and the progress of the conversion was followed by iodometric estimation of the unconsumed oxidant. The ΔH^\ddagger and ΔS^\ddagger were obtained through least square analysis of log k versus $1/T$ plots adopting the logarithmic form of Eyring relationship $\log_{10}(k/T) = 10.318 + (\Delta S^\ddagger/19.147T) - (\Delta H^\ddagger/19.147T)$.

Results and discussion

Aniline into azobenzene

SPB in glacial acetic acid, with catalytic amount of molybdenum(VI), effectively converts most of the anilines into azobenzenes, identified by their IR (Fig. S1–S43 in Supplementary material) and UV–visible spectra and melting points; the yields are good (see “Experimental” section).



Choice of solvent and catalyst

SPB dissolves in acetic acid (HOAc) readily and less so in ethylene glycol (EG) but insoluble in other organic solvents like 2-methoxy-pentan-2,3-diol, glycerol, ethanol, 2-ethoxyethanol, 2-butoxyethanol, methanol (MeOH), 2-propanol, *t*-butanol, dioxane, acetonitrile and dimethylformamide. While Mn(II), Fe(II), Ni(II), Cu(II), Cd(II), Sn(II), Pb(II), Sb(II) and Bi(III) fail to catalyze the reaction in acetic acid, Cr(VI), Co(II) and Pd(II) catalyze decomposition of SPB. Although Zr(IV) catalyzes the reaction, the kinetic results lack reproducibility. Many commercially available salts or oxoacids of transition or inner transition metals are insoluble in glacial acetic acid (see “Experimental” section).

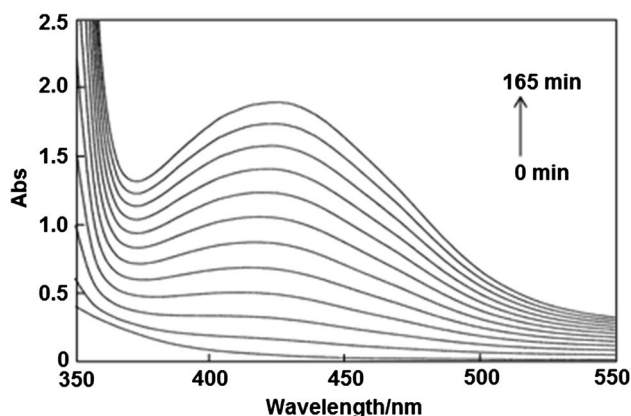


Fig. 1 UV-Vis spectral time scan of the reaction in acetic acid. $[\text{SPB}]_0 = 5.0 \text{ mM}$, $[\text{aniline}]_0 = 0.10 \text{ M}$, $[\text{Mo(VI)}] = 0.50 \text{ mM}$, 35°C

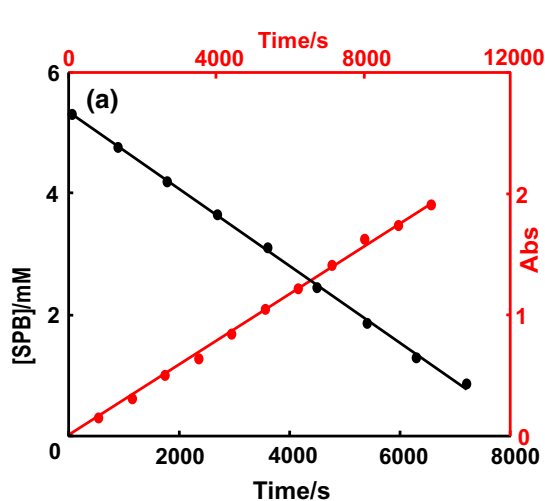
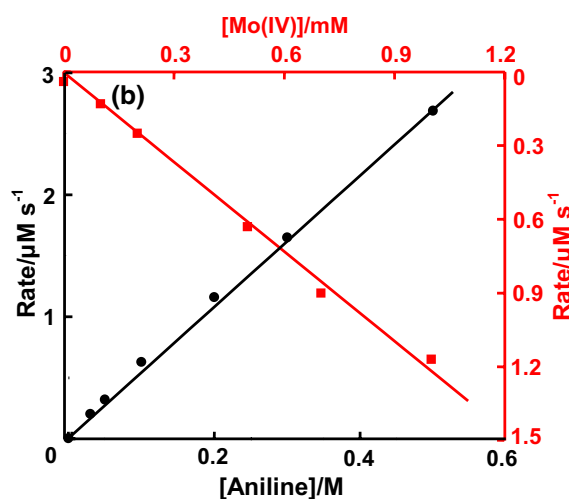


Fig. 2 a Linear decrease of $[\text{SPB}]$ or increase of $[\text{PhN=NPh}]$ with reaction time. $[\text{SPB}]_0 = 5.0 \text{ mM}$, $[\text{aniline}]_0 = 0.10 \text{ M}$, $[\text{Mo(VI)}] = 0.50 \text{ mM}$, solvent=HOAc, 35°C .

Kinetic orders

The uncatalyzed conversion of anilines into azobenzenes in glacial acetic acid by SPB is sluggish at room temperature, although it occurs at elevated temperatures (McKillop and Sanderson 1995; Muzart 1995). SPB in glacial acetic acid produces peracetic acid on aging and peracetic acid oxidizes aniline to azobenzene very much faster than SPB (Karunakaran and Kamalam 2002a). The Mo(VI)-catalyzed conversion of anilines to azobenzenes by SPB in glacial acetic acid was studied under the conditions: $[\text{aniline}] \gg [\text{SPB}] \gg [\text{Mo(VI)}]$ with fresh solution of SPB as well as Na_2MoO_4 in acetic acid; the catalyst was thrown out from Na_2MoO_4 solution in acetic acid on standing. The reaction was initiated through the addition of aniline to SPB and Na_2MoO_4 , all dissolved in acetic acid. The UV-Vis spectra of the reaction solution, recorded at different reaction times, show the formation of azobenzene (Fig. 1). The kinetics of the reaction was studied by iodometric estimation of the unconsumed oxidant at different time intervals. The reaction is zero order with respect to the oxidant; the oxidant concentration decreases linearly with reaction time, as shown by Fig. 2a. Also, the reaction rate does not differ significantly on increasing $[\text{SPB}]_0$ from 2 to 10 mM $[[\text{aniline}]_0 = 0.10 \text{ M}$, $[\text{Mo(VI)}] = 0.50 \text{ mM}$, 35°C , $\text{rate} = 0.64 \pm 0.01 \mu\text{M s}^{-1}$]. Not only the consumption of the oxidant but also the product formation is zero order; plot of absorbance (440 nm) vs. reaction time is linear almost through the origin (Fig. 2a). The conversion is first order with respect to aniline; the reaction rate increases linearly with $[\text{aniline}]_0$ (Fig. 2b). The decomposition of the oxidant is insignificant. Also, the reaction is first order with respect to Mo(VI), as evident from the linear plot of reaction rate vs. $[\text{Mo(VI)}]$ (Fig. 2b); the



on $[\text{aniline}]_0$ or $[\text{Mo(VI)}]$. $[\text{SPB}]_0 = 5.0 \text{ mM}$, solvent=HOAc, 35°C , $[\text{Mo(VI)}] = 0.50 \text{ mM}$ or $[\text{aniline}]_0 = 0.10 \text{ M}$

uncatalyzed reaction is sluggish. Trichloroacetic acid (TCA) suppresses the reaction rate. Addition of TCA [0.10 M in methanolic (60% v/v) acetic acid (40% v/v)] decreases the reaction rate from 0.16 to 0.071 $\mu\text{M s}^{-1}$ $[[\text{SPB}]_0 = 5.0 \text{ mM}, [\text{aniline}]_0 = 0.050 \text{ M}, [\text{Mo(VI)}] = 0.50 \text{ mM}, 35^\circ\text{C}]$. Further addition of TCA (0.20, 0.30, 0.40 and 0.50 M) does not have any significant effect. Acetic acid is the most suitable solvent for the reaction. The reaction is very slow in EG (Table S1). Addition of methanol or EG or water slows down the product formation. Moreover, dissolution of SPB in acetic acid or EG or water shows little difference in the kinetic results. Boric acid and borate do not influence the reaction rate in acetic acid (Table S2). The reaction in acetic acid does not proceed through a radical mechanism. Addition of vinyl monomer acrylamide or acrylonitrile neither leads to polymerization nor suppresses the reaction rate (Table S1). Furthermore, anionic surfactants like aerosol OT (AOT) and sodium lauryl sulfate (SLS) do not remarkably influence the conversion.

Mechanism

SPB on dissolution in glacial acetic acid affords H_2O_2 quantitatively and on aging, peracetic acid is formed at the expense of H_2O_2 (Karunakaran and Kamalam 2000, 2002a). In acetic acid, Na_2MoO_4 exists as MoO_3 , the coordinated water molecule omitted (Karunakaran and Muthukumar 1995). With H_2O_2 in acidic medium, MoO_3 forms

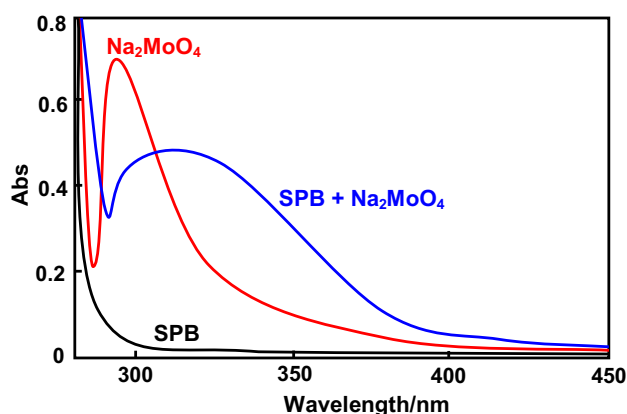
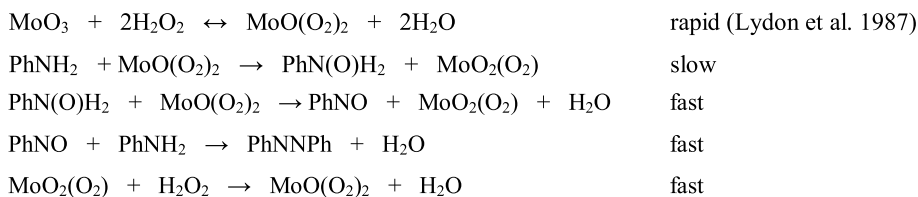


Fig. 3 UV-Vis spectral evidence of $\text{MoO}(\text{O}_2)_2$

oxodiperoxomolybdenum(VI) $[\text{MoO}(\text{O}_2)_2]$ (Lydon et al. 1987). As the reaction is rapid and the formation constant is very large, under the condition $[\text{H}_2\text{O}_2] \gg [\text{Mo(VI)}]$, the catalyst practically exists as $\text{MoO}(\text{O}_2)_2$ (Lydon et al. 1987). The zero order of the reaction with respect to the oxidant is in conformity with the same. The first-order dependence of the reaction rate on $[\text{Mo(VI)}]$ as well as $[\text{aniline}]$ points to oxidation of aniline by the reactive peroxo molybdenum(VI) species as slow and rate-limiting. UV-Vis spectroscopic study provides evidence of formation of oxodiperoxomolybdenum(VI). Figure 3 displays the UV-Vis spectra of (1) Na_2MoO_4 , (2) SPB and (3) SPB with Na_2MoO_4 , all dissolved in glacial acetic acid. While SPB does not absorb significantly in the UV-Vis region, Na_2MoO_4 absorbs at 292 nm. The UV-Vis spectrum of SPB dissolved in glacial acetic acid along with Na_2MoO_4 shows absorption at 309–323 nm. This is in agreement with the wavelength of absorption of $\text{MoO}(\text{O}_2)_2$, reported by Thompson and coworkers (328 nm in aqueous perchloric acid) (Lydon et al. 1987). Cyclic voltammetric study supports the basis of the reaction mechanism. While the solvent glacial acetic acid does not undergo reduction in the working potential range, fresh solution of SPB in acetic acid shows a cathodic peak at -31 mV (Figs. S44 and S45 in Supplementary material). Aging of SPB in glacial acetic acid is reflected in the cyclic voltammogram (CV) also; the cathodic peak potential is shifted from -31 to $+77 \text{ mV}$ on aging of SPB (Fig. S46 in Supplementary material). Further, aging of the catalyst molybdenum(VI) in glacial acetic acid, probably resulting in oligomerization of molybdenum(VI) species, is also reflected in the CV of fresh and aged solution of Na_2MoO_4 ; while the fresh solution does not show any significant reduction, the aged catalyst exhibits a cathodic peak at $+928 \text{ mV}$ (Fig. S47 and S48 in Supplementary material). Cyclic voltammetric results also support the formation of molybdenum(VI) peroxo species; the CV of SPB with Na_2MoO_4 exhibits a cathodic peak potential at $+128 \text{ mV}$ (Fig. S49 in Supplementary material). That is, addition of Na_2MoO_4 shifts the reduction potential of SPB by 159 mV (from -31 mV). Scheme 1 is the suggested detailed reaction sequence. Phenylhydroxyl amine has been suggested as an intermediate in some of the peroxo oxidation of anilines to azobenzenes (Karunakaran and Kamalam 2002a). The reported mechanism is the slow and rate-determining

Scheme 1

Scheme 1



oxidation of aniline to phenylhydroxyl amine followed by the fast oxidation of the latter to nitrosobenzene which couples with aniline to yield azobenzene. But in the title reaction, phenylhydroxyl amine is not an intermediate; oxidation of phenylhydroxyl amine by SPB in the presence of Mo(VI) is not fast. Experiments show that the rates of Mo(VI)-catalyzed SPB oxidation of phenylhydroxyl amine and aniline, under identical conditions, do not differ significantly (Fig. S50).

Solvent specificity

Well proved is the validity of linear solvation energy relationships (LSER) (Kamlet et al. 1983; Swain et al. 1983) and numerous reactions were found to conform to LSER in a variety of organic solvents (Vyas and Sharma 2002; Saraswat et al. 2003). The Taft LSER (Kamlet et al. 1983) is: $\log \text{rate} = A_0 + p\pi^* + b\beta + a\alpha$, where π^* is the solvent polarity for solvent–solute interaction of non-specific type, β refers to the solvent hydrogen-bond acceptor basicity and α represents the solvent hydrogen-bond donor acidity. Swain et al. (1983) LSER equation is: $\log \text{rate} = aA + bB + C$, where A and B are anion and cation solvating power of the solvent, respectively. As SPB is insoluble in most of the organic solvents, the reaction was conducted by adding different organic solvents to the reactants and catalyst dissolved in acetic acid; the composition of acetic acid in the reaction solution was 80% (v/v) and the added organic solvent was 20% (v/v). The stated solvent parameters of the reaction medium, like the relative permittivity (dielectric constant), were deduced adopting the principle of additivity (Table S3 in supplementary material). Analysis of the measured reaction rates in binary solvents (presented in Table S4) in terms of the stated LSERs shows no such correlation pointing out the solvent-specific nature of the title reaction.

Common mechanism

The structure of aniline, the substituent attached to the ring, determines the reactivity and the structure–reactivity relationships are well established (Hansch et al. 1991). The effect of substituent on the rate of aniline to azobenzene conversion by SPB in the presence of Mo(VI) has been studied with about 50 *para*-, *meta*- and *ortho*-substituted anilines. The activation parameters were calculated from the second-order rate constants [$k_2 = \text{rate}/[\text{aniline}]_0[\text{Mo(VI)}]$] at 20, 35 and 50 °C using the Eyring relationship by the method of least squares (Table 1). The conversion is not isoentropic; in an isoentropic reaction series, only the enthalpy of activation (ΔH^\ddagger) determines the reactivity. Neither the reaction is isoenthalpic. The reactivity in an isoenthalpic series is solely governed by the activation entropy (ΔS^\ddagger). On the other hand, compensation law exists (Liu and Guo 2001). It is the linear

relationship between ΔH^\ddagger and ΔS^\ddagger (Fig. 4a). The compensation effect occurs when the free energy of activation (ΔG^\ddagger) within the reaction series does not vary significantly, whereas the ΔH^\ddagger and ΔS^\ddagger do. Large experimental error also leads to false compensation (Liu and Guo 2001). The compensation effect and isokinetic effect are not synonymous, and the occurrence of one does not imply the occurrence of the other. The isokinetic relationship demands the existence of common intersection point of Arrhenius lines of a series of similar reactions. A simple method to evaluate the isokinetic relationship, suggested by Exner, is to plot the logarithms of rate constants at two different temperatures against each other. A linear plot implies a valid isokinetic relationship and conversion of anilines into azobenzenes by SPB in acetic acid with Mo(VI) as catalyst conforms to such a linear relationship (Fig. 4b). The validity of the isokinetic relationship implies operation of a common mechanism throughout the reaction series. The observation that *N*-methylaniline, *N,N*-dimethylaniline and diphenylaniline conform to the compensation law (Fig. 4a) and to the isokinetic relationship (Fig. 4b) supports the suggested rate-limiting step, the slow reaction of oxidoperoxomolybdenum(VI) with molecular anilines. As the fast reactions following the rate-limiting one do not fall under the requisites of the theories of reaction rates and linear free energy relationships, formation of different products does not preclude common mechanism up to the rate-determining step.

Correlation of reactivities

Table 1 shows that the variation of the reaction rate fails to commensurate with the very wide range of substituents employed. That is, the electron-releasing or demanding power of the substituents does not sufficiently reflect on the spread of the reaction rate. Further, the specific reaction rate (k_2) fails to conform to the usual Hammett relationship at any of the temperatures studied. Figure 5a is the scattergram resulting from Hammett's correlation of rate at 35 °C. The reaction center is likely to cross-conjugate with the *para*-substituents in aniline and correlation of reaction rates of (1) *para*-substituted and (2) *meta*-substituted anilines separately using Hammett (σ_p or σ_m) or Brown-Okamoto (σ_p^+ or σ_m^+) or modified Hammett (σ_p^-) relationship is unsuccessful (at any of the temperatures measured). Analysis of the reaction rates (at 20 or 35 or 50 °C) in terms of the dual substituent parameter (DSP) equations (*para*: $\sigma_p, \sigma_R; \sigma_p, \sigma_R^+; \sigma_p, \sigma_R^-; F, R$; *meta*: $\sigma_p, \sigma_R; \sigma_p, \sigma_R^+; \sigma_p, \sigma_R^-; F, R$) (Shorter 1991) fails to provide satisfactory correlation. The values of the substituent constants used are listed in Tables S5 and S6 in supplementary material. The Hammett relationship and its different modified forms are applicable to *para*- and *meta*-substituted benzene derivatives but not to the *ortho*-compounds; besides the well-known inductive and resonance effects associated with

Table 1 Second-order rate constants (k_2), activation parameters and specific reaction rates of molecular anilines (k_2^\ddagger) in acetic acid

Entry	Substituent	$10^2 k_2/\text{M}^{-1} \text{s}^{-1}$			$\Delta H^\ddagger/\text{kJ mol}^{-1}$	$-\Delta S^\ddagger/\text{J K}^{-1} \text{mol}^{-1}$	$k_2^\ddagger/\text{M}^{-1} \text{s}^{-1}$		
		20	35	50 °C			20	35	50 °C
1	H	0.225	1.17	4.60	76.7	33.5	0.279	1.45	5.70
2	<i>m</i> -CH ₃	0.174	1.07	4.28	81.5	19.0	0.277	1.70	6.80
3	<i>m</i> -OCH ₃	0.361	1.55	5.49	68.8	56.6	0.182	0.784	2.77
4	<i>m</i> -OH ^a	2.21	13.1	72.1 [#]	88.8	-26.5	1.43	8.48	46.5
5	<i>m</i> -Cl	0.303	1.42	4.74	69.7	55.0	0.0365	0.172	0.572
6	<i>m</i> -Br	0.505	1.44	4.12	52.5	110	0.0621	0.177	0.507
7	<i>m</i> -NO ₂	0.312	1.28	5.21	71.3	49.7	0.00774	0.0317	0.129
8	<i>m</i> -COOH	0.454	2.95	14.7	88.7	-13.0	0.0246	0.160	0.794
9	<i>m</i> -COCH ₃	0.616	2.83	6.19	58.2	87.7	0.0803	0.369	0.807
10	<i>m,p</i> -(CH ₃) ₂	0.131	0.717	3.23	81.5	21.8	0.596	3.26	14.7
11	<i>m,p</i> -Cl ₂	0.471	2.51	7.41	69.9	50.2	0.0215	0.115	0.339
12	<i>p</i> -CH ₃	0.478	1.94	10.4	78.0	23.4	1.77	7.19	38.5
13	<i>p</i> -OCH ₃	0.197	0.910	5.57	84.9	7.54	1.39	6.40	39.2
14	<i>p</i> -OC ₂ H ₅	0.186	0.789	3.25	72.4	50.2	1.02	4.31	17.7
15	<i>p</i> -SO ₃ H	insoluble							
16	<i>p</i> -NH ₂	22.2	-	-	-	-	0.965	-	-
17	<i>p</i> -Cl	0.581	3.18	12.9	78.8	18.6	0.185	1.02	4.11
18	<i>p</i> -Br	0.351	1.75	7.78	78.7	23.3	0.0884	0.440	1.96
19	<i>p</i> -I	0.766	2.69	9.64	63.9	67.6	0.170	0.598	2.14
20	<i>p</i> -NO ₂	0.111	0.415	1.94	72.4	54.8	0.00132	0.00495	0.232
21	<i>p</i> -COOH	0.277	0.938	3.59	64.5	73.9	0.00655	0.0222	0.0850
22	<i>p</i> -COOC ₂ H ₅	0.458	1.17	4.08	54.6	104	0.0119	0.0304	0.106
23	<i>p</i> -COCH ₃	0.275	0.761	2.39	54.0	110	0.00943	0.0261	0.0820
24	<i>p</i> -NHCOCCH ₃	0.280	1.61	6.49	80.0	20.4	0.211	1.22	4.90
25	<i>p</i> -SO ₂ NH ₂	0.265	1.28	3.56	65.8	68.9	0.0353	0.171	0.474
26	<i>o,m</i> -(CH ₃) ₂ (2, 3)	0.241	1.02	4.34	73.2	45.2	0.375	1.59	6.75
27	<i>o,m</i> -(CH ₃) ₂ (2, 5)	0.491	1.55	6.29	64.2	70.3	0.519	1.64	6.66
28	<i>o,m</i> -(OCH ₃) ₂ (2, 5) ^b	2.26	8.68	31.0 [#]	66.2	50.5	0.633	2.43	8.70
29	<i>o,m</i> -Cl ₂ (2, 3)	0.153	0.579	1.47	57.0	104	0.00232	0.00878	0.0223
30	<i>o,m</i> -Cl ₂ (2, 5)	0.100	0.376	1.22	63.0	87.1	0.00137	0.00516	0.0167
31	<i>o,p</i> -Cl ₂	0.222	0.785	2.68	62.7	81.7	0.00383	0.0136	0.0463
32	<i>o,o,p</i> -Cl ₃	0.047	0.249	0.779	71.3	64.6	0.000496	0.00263	0.00822
33	<i>o,o,p</i> -Br ₃	0.235	0.758	2.92	63.4	79.1	0.0027	0.00871	0.0336
34	<i>o</i> -CH ₃	0.290	1.14	4.83	71.1	50.9	0.256	1.01	4.27
35	<i>o</i> -OCH ₃	0.175	0.987	2.62	68.7	62.3	0.185	1.04	2.77
36	<i>o</i> -OC ₂ H ₅	0.356	1.02	3.24	55.2	103	0.329	0.942	2.99
37	<i>o</i> -OC ₆ H ₅	0.711	1.93	5.63	51.6	110	0.0298	0.0808	0.236
38	<i>o</i> -OH ^c	13.0	44.2	244	74.0	10.1	18500	62800	347000
39	<i>o</i> -Cl	0.223	0.757	2.11	56.4	103	0.00669	0.0227	0.0633
40	<i>o</i> -Br	0.241	0.899	2.29	56.7	101	0.00642	0.0239	0.0610
41	<i>o</i> -NO ₂	0.107	0.188	0.507	38.0	173	0.00111	0.00196	0.00528
42	<i>o</i> -COOH	0.140	0.549	2.33	71.1	57.0	0.00256	0.0101	0.0427
43	<i>o</i> -COOCH ₃	0.158	0.664	1.95	63.5	81.3	0.00357	0.0150	0.0441
44	<i>o</i> -NH ₂ ^d	1.32	7.60	38.5 [#]	86.0	12.7	0.0338	0.195	0.987
45	<i>o</i> -SH	fast							
46	<i>o,o</i> -(NO ₂) ₂	-	-	0.144	-	-	-	-	0.00144
47	-NHCH ₃ ^e	4.73	15.9	49.1 [#]	58.8	69.5	10.3	34.8	107
48	-N(CH ₃) ₂	0.444	1.63	5.31	62.5	76.5	1.93	7.10	23.1
49	-NHC ₆ H ₅	0.263	0.857	2.85	60.0	89.9	0.00307	0.0100	0.0333

[SPB]₀ = 10 mM, [aniline]₀ = 0.10 M, [Mo(VI)] = 1.0 mM[#]Extrapolated values: ^a5.31 × 10⁻³ M⁻¹ s⁻¹ at 10 °C, ^b7.87 × 10⁻³ M⁻¹ s⁻¹ at 10 °C, ^d3.52 × 10⁻³ M⁻¹ s⁻¹ at 10 °C, ^e1.88 × 10⁻² M⁻¹ s⁻¹ at 10 °C^c[aniline]₀ = 0.02 M

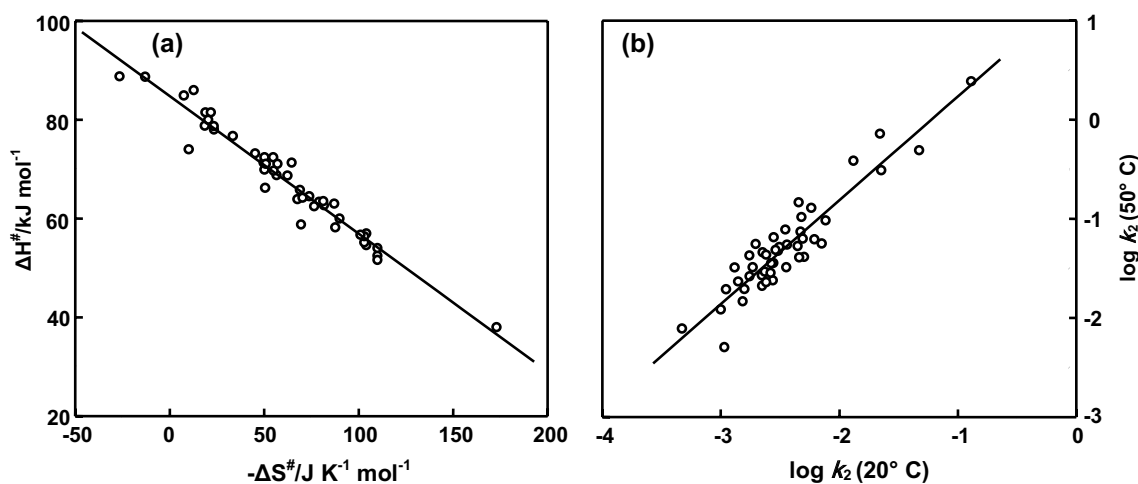


Fig. 4 a The compensation effect. b The Exner plot

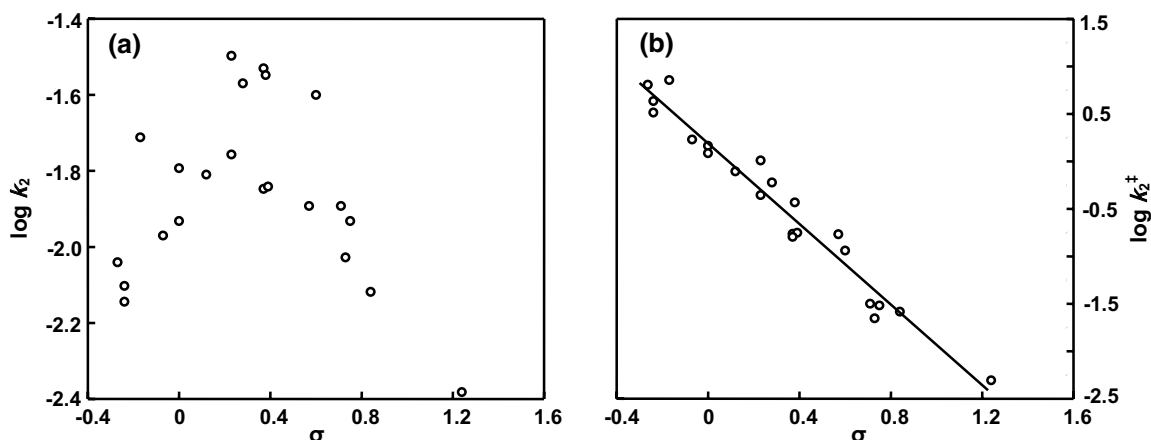


Fig. 5 a The Hammett plot. b The Hammett plot employing rate constants of molecular anilines

the *para*- and *meta*-substituents, the *ortho*-substituents cause steric effect. The determined ΔH^\ddagger and ΔS^\ddagger of the reactions of all the *para*-, *meta*- and *ortho*-substituted anilines conform to the isokinetic relationship (Fig. 4a). So are the measured reaction rates at two extreme temperatures (Fig. 4b). This indicates that the reaction mechanism of *ortho*-substituted anilines is not different from that of *para*- and *meta*-substituted anilines and justifies the analysis of reaction rates of *ortho*-substituted anilines in terms of the structure–reactivity relationship. The reaction rates of *ortho*-substituted anilines also fail to conform to Charton's LDS (localized, delocalized, steric) equation (Aslam et al. 1981); the carboxy, nitro and methoxycarbonyl substituents individually take either planar or orthogonal orientation, requiring appropriate steric substituent constants (ν).

Reactions of anilines in non-aqueous, basic, neutral and acidic media (26 in number), as listed by Karunakaran and Kamalam (2002b), are reported to conform to

structure–reactivity relationship. In non-aqueous, basic and neutral media, anilines stay as free bases (molecular anilines), whereas in acidic medium, they exist in dual form—free bases and conjugate acids. The acidity of the medium and the pK_a (of aniline) determine the relative abundance of the two forms ($[\text{PhNH}_2]/[\text{PhNH}_3^+]$). So far, the substrate-independent specific reaction rates ($=k_0/[\text{aniline}]_0$ or $k'/[\text{aniline}]_0$, where k_0 and k' are pseudo-zero-order and pseudo-first-order rate constants under the condition aniline concentration is in large excess over other reactants) were deduced employing the total concentration of aniline ($[\text{PhNH}_2] + [\text{PhNH}_3^+] = [\text{aniline}]_T$ or $[\text{aniline}]_0$) in the reaction solution. Since the pK_a varies from 5.36 (*p*-OCH₃) to -5.23 [*o,o*-(NO₂)₂] and molecular anilines are vulnerable to oxidation than the anilinium ions, the reported $k_0/[\text{aniline}]_0$ and $k'/[\text{aniline}]_0$ are not the real specific reaction rates. Hence, the so far reported structure–reactivity correlation employing $k_0/[\text{aniline}]_0$ or $k'/[\text{aniline}]_0$ is erroneous. The

real specific reaction rates are to be deduced using molecular aniline concentration ($[\text{PhNH}_2]$) and not $[\text{aniline}]_0$. The concentration of free bases may be deduced from the acid strength of the medium and the pK_a values of the anilines and acetic acid (Perrin 1965; Dean 1987; Buckingham et al. 1996). Although the pK_a values are associated with aqueous solutions, an in depth examination shows that they may be employed to deduce the concentrations of free bases in glacial acetic acid. Coupling acetic acid-ionization equilibrium with that of anilinium ion eliminates $[\text{H}_2\text{O}]$ and $[\text{H}_3\text{O}^+]$. The ratio of ionization constants of acetic acid and anilinium ion provides the equilibrium constant of the reaction $\text{PhNH}_2 + \text{HOAc} \leftrightarrow \text{PhNH}_3^+ + ^-\text{OAc}$. In the absence of water, self-ionization of HOAc is unlikely, and hence $[\text{PhNH}_3^+] = [^-\text{OAc}]$. Solving the said equations provides $[\text{PhNH}_2]$. The specific reaction rates ($k_2^\ddagger = k_0/[\text{PhNH}_2]$ $[\text{Mo(VI)}]$), thus deduced and presented in Table 1, conform to the usual Hammett relationship at all the temperatures studied. Figure 5b is the Hammett plot at 35 °C (correlation coefficient, $r = 0.94$, standard deviation, $\text{sd} = 0.32$, number of data points, $n = 23$, reaction constant, $\rho = -2.22$ at 20–50 °C). The plots involve the ordinary benzoic acid-based σ values and include *p*-nitro, *p*-ethoxycarbonyl, and *p*-carboxy substituents. In anilines, these substituents enter into cross-conjugation with the reaction center and withdraw electron strongly through resonance, necessitating the use of σ_p^- (Fig. 5b).

m-Aminophenol exhibits very high reactivity and does not conform to the structure–reactivity relationship. A possible reason is assistance of hydroxyl group in the reaction process. It may be, initial binding of $\text{MoO}(\text{O}_2)_2$ with *m*-OH function followed by the oxygen transfer. Attack on amino nitrogen by $\text{MoO}(\text{O}_2)_2$ with neighbouring hydroxyl group participation may also enhance the reactivity of aminophenol. *p*-Phenylenediamine in glacial acetic acid may exist in three forms, viz., $p\text{-}^+\text{H}_3\text{NC}_6\text{H}_4\text{NH}_3^+$, $p\text{-}^+\text{H}_3\text{NC}_6\text{H}_4\text{NH}_2$ and $p\text{-H}_2\text{NC}_6\text{H}_4\text{NH}_2$. Calculation using the pK_a (+1) value of *p*-phenylenediamine, pK_a of acetic acid and the acidity of the medium shows that the concentration of the free base is negligible (0.03%). Further, calculation using the pK_a (+2) value of the amine reveals that it exists largely in diprotonated form (77%) and significantly in monoprotated form (23%). The specific reaction rate of $p\text{-}^+\text{H}_3\text{NC}_6\text{H}_4\text{NH}_2$ was obtained using its concentration in the reaction medium; the method adopted for other anilines is not applicable to the diamine as it exists in three forms. $p\text{-}^+\text{H}_3\text{NC}_6\text{H}_4\text{NH}_2$ as the reactive substrate results in protonated amino group ($-\text{NH}_3^+$) as the substituent which is highly electron demanding ($\sigma_p = 0.60$). The deduced specific rate does not reflect the same, and fails to fit the Hammett line. A possible reason is complication due to the parallel reaction of the highly reactive free base ($p\text{-H}_2\text{NC}_6\text{H}_4\text{NH}_2$) present in trace (0.03%) in the reaction medium. $p\text{-}^+\text{H}_3\text{NC}_6\text{H}_4\text{NH}_2$ and

$p\text{-H}_2\text{NC}_6\text{H}_4\text{NH}_2$ are at rapid equilibrium which supplies the free base at a steady concentration. As the protonated amino group ($-\text{NH}_3^+$) is highly electron withdrawing, the ΔG^\ddagger of the reaction of $p\text{-}^+\text{H}_3\text{NC}_6\text{H}_4\text{NH}_2$ is likely to be large leading to slow conversion.

The specific reaction rates of *ortho*-substituted molecular anilines (free bases) have been analyzed in terms of Charton's LDS equation. The reaction of *o*-aminophenol is fast; it is likely to enter into intra-molecular H-bonding. Like *m*-OH, *o*-OH may also bind with $\text{MoO}(\text{O}_2)_2$ prior to oxygen transfer to the amino group. In glacial acetic acid, *o*-phenylenediamine, like *p*-phenylenediamine, may exist in three forms, viz., diprotonated, monoprotated and unprotonated species. Calculation shows $o\text{-}^+\text{H}_3\text{NC}_6\text{H}_4\text{NH}_3^+$ as predominant species (59.6%) and $o\text{-H}_2\text{NC}_6\text{H}_4\text{NH}_2$ in trace (1.1%) with $o\text{-}^+\text{H}_3\text{NC}_6\text{H}_4\text{NH}_2$ at 39.3%. The reaction rate of $o\text{-}^+\text{H}_3\text{NC}_6\text{H}_4\text{NH}_2$ has been deduced using its concentration in glacial acetic acid. The specific reaction rates of *ortho*-substituted molecular anilines, excluding aminophenol and phenylenediamine, satisfactorily conform to Charton's LDS equation ($R^2 = 0.97\text{--}0.99$); each dataset involves ten substituents, viz., methyl, methoxy, ethoxy, phenoxy, chloro, bromo, nitro, carboxy, methoxycarbonyl and hydrogen. The conformity of the deduced reaction rates of molecular anilines to LFER shows operation of a common mechanism in the Mo(VI) -catalyzed oxidative dehydrogenative coupling of anilines yielding azobenzenes using SPB as oxygen source in acetic acid.

Conclusion

A large number of anilines are converted into azobenzenes under mild conditions in good yield using cheap, stable, innocuous, commercially available and industrial manufactured SPB with non-toxic Na_2MoO_4 in trace as catalyst. Glacial acetic acid is the solvent of choice. This method is commercially viable as it requires neither precious metal nanoparticles as catalyst (the recovery of which is a challenge) nor uneconomical oxygen source for the reaction. Furthermore, boric acid and molybdenum(VI), the reaction wastes, are micronutrients for plants which address the environmental concern. The determined kinetic orders of the conversion along with the UV–visible spectroscopic and cyclic voltammometric results suggest reaction of $\text{MoO}(\text{O}_2)_2$ with molecular aniline as slow and rate limiting. The enthalpies and entropies of activation of the oxidation of anilines, about 50 in number, conform to the compensation effect and the reaction rates to Exner's relationship. While oxidations of anilines yielding mixture of products are reported to conform to LFER, the titled reaction rates, deduced adopting the conventional method, fail to comply with the Hammett

relationship. However, the reaction rates of molecular anilines (free aniline base), obtained by a modified method, conform to the usual Hammett linear free energy relationship, indicating the flaw in the method of calculation adopted so far. Thus, the determined reaction constant allows prediction of the true rate of conversion of any aniline into corresponding azobenzene using $\text{Na}_2\text{MoO}_4/\text{SPB}$ in acetic acid and enables to arrive at the observable experimental reaction rate through reverse calculation.

References

- Almohareb T (2017) Management of discolored endodontically treated tooth using sodium perborate. *J Int Oral Health* 9:133–135. https://doi.org/10.4103/jioh.jioh_131_17
- Aslam MH, Burdon AG, Chapman NB, Shorter J, Charton M (1981) The separation of polar and steric effects. Part 14. Kinetics of the reactions of benzoic acid and of ortho-substituted benzoic acids with diazodiphenylmethane in various alcohols. *J Chem Soc Perkin Trans 2*:500–508. <https://doi.org/10.1039/P29810000500>
- Buckingham J (1995) Dictionary of organic compounds. Chapman & Hall/CRC, London
- Buckingham J, Donaghy SM, Cadogan JIG, Raphael RA, Roes CW (1996) Dictionary of organic compounds. Chapman & Hall, London
- Cai S, Rong H, Yu X, Liu X, Wang D, He W, Li Y (2013) Room temperature activation of oxygen by monodispersed metal nanoparticles: oxidative dehydrogenative coupling of anilines for azobenzene syntheses. *ACS Catal* 3:478–486. <https://doi.org/10.1021/cs300707y>
- Cvijetic IN, Vitorovic-Todorovic MD, Juranic IO, Drakulic BJ (2013) Reactivity of (*E*)-4-aryl-4-oxo-2-butenic acid arylamides toward 2-mercaptoethanol. A LFER study. *Monatsh Chem* 144:1815–1824. <https://doi.org/10.1007/s00706-013-1084-6>
- Dean JA (1987) Handbook of organic chemistry. McGraw-Hill, New York
- Dutta B, Biswas S, Sharma V, Savage NO, Alpay SP, Suib SL (2016) Mesoporous manganese oxide catalyzed aerobic oxidative coupling of anilines to aromatic azo compounds. *Angew Chem Int Ed* 55:2171–2175. <https://doi.org/10.1002/anie.201508223>
- Gao BB, Zhang M, Chen XR, Zhu DL, Yu H, Zhang WH, Lang JP (2018) Carbon-based AuAg alloy nanoparticles via the heterometallic $[\text{Au}_4\text{Ag}_4]$ cluster approach for efficient oxidative coupling of anilines. *Dalton Trans* 47:5780–5788. <https://doi.org/10.1039/C8DT00695D>
- Grierrane A, Corma A, Garcia H (2008) Gold-catalyzed synthesis of aromatic azo compounds from anilines and nitroaromatics. *Science* 322:1661–1664. <https://doi.org/10.1126/science.1166401>
- Hansch C, Leo A, Taft RW (1991) A survey of Hammett substituent constants and resonance and field parameters. *Chem Rev* 91:165–195. <https://doi.org/10.1021/cr00002a004>
- Indi YM, Wasif A, Patel AA (2017) Activated bleaching with sodium perborate and potassium persulphate. *Indian J Fibre Text Res* 42:235–240. <http://nopr.niscair.res.in/handle/123456789/42052>
- Jasinski R, Kwiatkowska M, Baranski A (2012) Kinetics of the [4 + 2] cycloaddition of cyclopentadiene with (*E*)-2-aryl-1-cyano-1-nitroethenes. *Monatsh Chem* 143:895–899. <https://doi.org/10.1007/s00706-012-0735-3>
- Kamlet MJ, Abboud JLM, Abraham MH, Taft RW (1983) Linear solvation energy relationship. 23. A comprehensive collection of the solvatochromic parameters, π^* , α , and β and some methods for simplifying the generalized solvatochromic equation. *J Org Chem* 48:2877–2887. <https://doi.org/10.1021/jo00165a018>
- Karunakaran C, Kamalam R (2000) On the mechanism of the perborate oxidation of organic sulphides in glacial acetic acid. *Eur J Org Chem*. [https://doi.org/10.1002/1099-0690\(200010\)2000:19<3261:AID-EJOC3261>3.0.CO;2.0](https://doi.org/10.1002/1099-0690(200010)2000:19<3261:AID-EJOC3261>3.0.CO;2.0)
- Karunakaran C, Kamalam R (2002a) Mechanism and reactivity in perborate oxidation of anilines in acetic acid. *J Chem Soc Perkin Trans 2*:2011–2018. <https://doi.org/10.1039/b208199g>
- Karunakaran C, Kamalam R (2002b) Structure–reactivity correlation of anilines in acetic acid. *J Org Chem* 67:1118–1124. <https://doi.org/10.1021/jo0158433>
- Karunakaran C, Muthukumar B (1995) Molybdenum(VI) catalysis of perborate or hydrogen peroxide oxidation of iodide ion. *Transit Met Chem* 20:460–462. <https://doi.org/10.1007/BF00141517>
- Karunakaran C, Venkataramanan R (2006a) Mo(VI)-catalysis of perborate oxidation in acetic acid: oxidation of dimethyl and dibenzyl sulfoxides. *Catal Comm* 7:236–239. <https://doi.org/10.1016/j.catcom.2005.09.016>
- Karunakaran C, Venkataramanan R (2006b) Mo(VI)-catalysis of perborate oxidation of aryl sulphides in acetic acid. *J Chem Res*. <https://doi.org/10.3184/030823406776894120>
- Liu L, Guo QX (2001) Isokinetic relationship, isoequilibrium relationship, and enthalpy–entropy compensation. *Chem Rev* 101:673–696. <https://doi.org/10.1021/cr990416z>
- Lydon JD, Schwane LM, Thompson RC (1987) Equilibrium and kinetic studies of the peroxo complex of molybdenum(VI) in acidic perchlorate solution. *Inorg Chem* 26:2606–2612. <https://doi.org/10.1021/ic00263a012>
- Ma H, Li W, Wang J, Xiao G, Gong Y, Qi C, Feng Y, Li X, Bao Z, Cao W, Sun Q, Veaceslav C, Wang F, Lei Z (2012) Organocatalytic oxidative dehydrogenation of aromatic amines for the preparation of azobenzenes under mild conditions. *Tetrahedron* 68:8358–8366. <https://doi.org/10.1016/j.tet.2012.07.012>
- McKillop A, Sanderson WR (1995) Sodium perborate and sodium percarbonate: cheap, safe and versatile oxidizing agents for organic synthesis. *Tetrahedron* 51:6145–6166. [https://doi.org/10.1016/0040-4020\(95\)00304-Q](https://doi.org/10.1016/0040-4020(95)00304-Q)
- Merino E (2011) Synthesis of azobenzenes: the coloured pieces of molecular materials. *Chem Soc Rev* 40:3835–3853. <https://doi.org/10.1039/c0cs00183j>
- Muzart J (1995) Sodium perborate and sodium percarbonate in organic synthesis. *Synthesis*, pp 1325–1347. <https://doi.org/10.1055/s-1995-4128>
- Paris E, Bigi F, Cauzzi D, Maggi R, Maestri G (2018) Oxidative dimerization of anilines with heterogeneous sulfonic acid catalysts. *Green Chem* 20:382–386. <https://doi.org/10.1039/C7GC03060F>
- Perrin DD (1965) Dissociation constants of organic bases in aqueous solution. Butterworths, London
- Salter-Blanc AJ, Bylaska EJ, Lyon MA, Ness SC, Tratnyek PG (2016) Structure–activity relationships for rates of aromatic amine oxidation by manganese dioxide. *Environ Sci Technol* 50:5094–5102. <https://doi.org/10.1021/acs.est.6b00924>
- Saraswat S, Sharma V, Banerji KK (2003) Kinetics and mechanism of oxidation of aliphatic primary alcohols by quinolinium bromochromate. *Proc Indian Acad Sci (Chem Sci)* 115:75–82. <https://www.ias.ac.in/article/fulltext/jcsc/115/01/0075-0082>
- Seth K, Roy SR, Kumar A, Chakraborti AK (2016) The palladium and copper contrast: a twist to products of different chemotypes and altered mechanistic pathways. *Catal Sci Technol* 6:2892–2896. <https://doi.org/10.1039/C6CY00415F>
- Shorter J (1991) In: Zalewski RI, Krygowski TM, Shorter J (eds) Similarity models in organic chemistry, biochemistry and related fields. Elsevier, Amsterdam

- Sun S, Liu Y, Ma J, Pang S, Huang Z, Gu J, Gao Y, Xue M, Yuan Y, Jiang J (2018) Transformation of substituted anilines by ferrate(VI): kinetics, pathways, and effect of dissolved organic matter. *Chem Eng J* 332:245–252. <https://doi.org/10.1016/j.cej.2017.08.116>
- Swain CG, Swain MS, Powell AL, Alunni S (1983) Solvent effects on chemical reactivity. Evaluation of anion- and cation-solvation components. *J Am Chem Soc* 105:502–513. <https://doi.org/10.1021/ja00341a033>
- Takada Y, Okumura S, Minakata S (2012) Oxidative dimerization of aromatic amines using *t*-BuOI: entry to unsymmetric aromatic azo compounds. *Angew Chem Int Ed* 51:7804–7808. <https://doi.org/10.1002/anie.201202786>
- Tran L, Orth R, Parashos P, Tao Y, Tee CWJ, Thomas VT, Towers G, Truong DT, Vinen C, Reynolds EC (2017) Depletion rate of hydrogen peroxide from sodium perborate bleaching agent. *J Endod* 43:472–476. <https://doi.org/10.1016/j.joen.2016.10.043>
- Vyas S, Sharma PK (2002) Kinetics and mechanism of the oxidation of organic sulphides by 2,2'-bipyridinium chlorochromate. *Proc Indian Acad Sci (Chem Sci)* 114:137–148. <https://doi.org/10.1007/BF02704306>
- Yamada S, Bessho J, Nakasato H, Tsutsumi O (2018) Color tuning donor-acceptor-type azobenzene dyes by controlling the molecular geometry of the donor moiety. *Dyes Pigment* 150:89–96. <https://doi.org/10.1016/j.dyepig.2017.11.002>
- Zhang C, Jiao N (2010) Copper-catalyzed aerobic oxidative dehydrogenative coupling of anilines leading to aromatic azo compounds using dioxygen as an oxidant. *Angew Chem Int Ed* 49:6174–6177. <https://doi.org/10.1002/anie.201001651>
- Zhu Y, Shi Y (2013) Facile Cu(I)-catalyzed oxidative coupling of anilines to azo compounds and hydrazines with diaziridinone under mild conditions. *Org Lett* 15:1942–1945. <https://doi.org/10.1021/ol4005917>